Available online at www.sciencedirect.com
ScienceDirect
Polymer 48 (2007) 290–301
polymer
www.elsevier.com/locate/polymer

Structure–property relationships and melt rheology of segmented, non-chain extended polyureas: Effect of soft segment molecular weight

Sudipto Das [a], Iskender Yilgor [b], Emel Yilgor [b], Bora Inci [b], Ozgul Tezgel [b], Frederick L. Beyer [c], Garth L. Wilkes [a,*]

[a] *Department of Chemical Engineering, Virginia Polytechnic Institute and State University, Blacksburg, VA 24061-0211, United States*
[b] *Department of Chemistry, Koc University, Istanbul, Turkey*
[c] *U.S. Army Research Laboratory, Aberdeen Proving Grounds, MD 21005, United States*

Received 4 August 2006; received in revised form 12 October 2006; accepted 13 October 2006
Available online 20 November 2006

Abstract

Novel, segmented non-chain extended polyureas were synthesized. Soft segments (SS) were based on poly(tetramethylene glycol) (PTMO) (average molecular weight 1000 or 2000 g/mol) and hard segments (HS) were based on a single molecule of a diisocyanate, which was either 1,6-hexamethylene diisocyanate (HDI), 1,4-phenylene diisocyanate (*p*PDI) or 1,4-*trans*-cyclohexyl diisocyanate (CHDI). An increase in the SS molecular weight was found to lead to an increased formation of SS crystallites below 0 °C, which increased the low temperature modulus. Both 1K and 2K PTMO-based polyureas showed a microphase separated morphology, where the HS formed thread-like, crystalline structures that were dispersed in the continuous SS matrix. Upon deformation, the HS were found to breakdown into distinctly smaller threads, which oriented along the direction of the strain; this effect was found to be partially reversible and time dependent. Both the 1K and 2K polyureas based on HDI HS were found to be thermally stable and potentially melt-processible.

Keywords: Polyurea; Block/segmented copolymers; Thermoplastic elastomers

1. Introduction

Segmented block copolymers consist of alternate hard and soft segments along their backbone. While the variously utilized soft segments (SS) have glass transition temperatures (T_g) below ambient temperature and provide flexibility, the hard segment (HS) domains function both as a reversible physical crosslink and as a reinforcing filler. In their service temperature window, these systems generally possess a microphase separated morphology, where (at low HS content) the HS are typically randomly dispersed as isolated microdomains in a continuous SS matrix [1]. The microphase separated morphology arises due to the chemical incompatibility between the HS and the SS (macrophase separation is prevented due to the covalent linkages between HS and SS) and the crystallizability of the HS. With an increase in HS content (generally at a HS content of over 25 wt%), the connectivity between the hard domains increases, ultimately becoming percolated throughout the SS matrix [2].

The most commonly used soft segment (SS) components include diol or diamine-terminated polyesters (e.g. polycaprolactone), polyethers [e.g. poly(ethylene oxide), poly(propylene oxide) (PPO), poly(tetramethylene oxide) (PTMO)], and polycarbonates [e.g. hexamethylene polycarbonate (PC)]. The conventional HS consist of diisocyanates and a chain-extender (CE). Commonly used diisocyanates include 4,4′-dicyclohexylmethane diisocyanate (HMDI), 1,4-diphenylmethane diisocyanate (MDI), toluene diisocyanate (TDI), *para*-phenylene diisocyanate (*p*PDI), etc. Most commonly used CEs are low molecular weight diamines [e.g. ethylenediamine (EDA)] for polyureas and low molecular weight diols [e.g. 1,4-butanediol (BD)] for polyurethanes [3–5].

* Corresponding author. Tel.: +1 540 231 5498; fax: +1 540 231 9511.
E-mail address: gwilkes@vt.edu (G.L. Wilkes).

0032-3861/$ - see front matter © 2006 Elsevier Ltd. All rights reserved.
doi:10.1016/j.polymer.2006.10.029

Segmented polyureas, polyurethanes or polyurethane–ureas are commonly synthesized by a two-step process, called the ''prepolymer'' method, where the first step consists of preparing an isocyanate terminated prepolymer through the reaction of soft segment oligomers with excess diisocyanate. This is followed by the reaction of the prepolymer mixture with stoichiometric amounts of a difunctional CE to form a high molecular weight polyurethane, polyurethane–urea or polyurea [3]. Three of the most important commercially available segmented copolymers used as thermoplastic elastomers (TPE) are polyurethane [ESTANE®], poly-(ether-*block*-ester) [HYTREL®] and poly(ether-*block*-amide) [PEBAX®]. Segmented polyureas and polyurethane–ureas [LYCRA®] are known to be difficult to melt process without thermal degradation, due to the highly cohesive nature of their bidentate hydrogen bonding between urea linkages, thereby limiting melt processibility. In this paper, we introduce novel segmented, non-chain extended polyureas which, as the preliminary melt rheology data indicate, may be melt processed using conventional techniques like extrusion or injection molding.

There is a widely held opinion in the industrial TPE sector that in order to obtain microphase separation in segmented copolymers with useful structural properties, the HS should be lengthened by the incorporation of a CE. Thus, very few studies have been done in the past on segmented, non-chain extended polyurethanes or polyureas. Yilgor et al. [6,7] as well as Tyagi et al. [8,9] were the first to synthesize [6,7] and investigate the structure–property behavior [8,9] of non-chain extended, segmented polyureas by reacting telechelic, amine-terminated polydimethylsiloxane (PDMS) oligomers with different diisocyanates such as MDI, TDI and HMDI. Though direct visual evidence of the microphase separation within these systems was not obtained, indirect evidence was presented in the form of dynamic mechanical analysis (DMA) [9], thermomechanical analysis (TMA) [6], small-angle X-ray scattering (SAXS) [8] and differential scanning calorimetry (DSC) [9] analysis. But the upper service temperature of these microphase separated copolymers was ca. 50 °C, limiting their commercial utility [8]. Colombani et al. [10] also synthesized non-chain extended, ''three-dimensional crosslinked'' thermoplastic elastomers based on bis-urea grafted PDMS polymers, which were synthesized by the reaction of amino-functionalized PDMS by mono-isocyanates. Relative to their amino-functional precursors, the grafted PDMS materials were shown to possess better tensile and rheological properties and could also be processed at high temperatures. Gaymans et al. [11–13] have studied segmented block copolymers based on PTMO SS and HS based on well-defined, crystallizable diester diamide units (2 nm long) [12]. These systems were shown to possess better elastic properties than some commercial materials [11]. AFM characterization of the copolymers showed the presence of a ribbon-like crystalline morphology [13]. Upon deformation, the ribbon-like crystallites irreversibly broke down into smaller units and oriented parallel to the stretch direction. Recently, Versteegen et al. [14,15] synthesized block copoly(ether urea)s with uniform hard segments based on PTMO oligomers. The authors studied the effects of size of the HS and number of urea groups in the HS on the properties of the segmented copolymers. Their results showed that the copolymers containing two urea groups per HS gave the optimum balance between excellent structural properties and ease of flow [15].

Over the past few years, our group has also been involved in the preparation and investigation of the structure–property relationships of novel, segmented polyurethanes and polyureas with the HS based on a single diisocyanate molecule, *without using CEs*, thereby providing two urea linkages per HS [16–18]. In these studies equimolar amounts of a diisocyanate were reacted with either a dihydroxy ($M_n = 975$ g/mol) or diamine ($M_n = 1100$ g/mol) terminated poly(tetramethylene oxide) to form a segmented polyurethane or polyurea, respectively [18], which contained only ~13% HS. Our results indicated that the symmetry of the diisocyanate and the nature of hydrogen bonding (monodentate or bidentate) have a pronounced effect on the microphase separated morphology and mechanical properties of these novel polyurethanes and polyureas [16–18]. One of our studies also showed that some potentially melt-processible, structural polyureas could be synthesized without the traditional use of chain extension by careful selection of the level of symmetry and hydrogen-bonding capacity [16].

In the present study, the effect of soft segment molecular weight on the structure–property relationships of some selected segmented, non-chain extended polyureas is further discussed. Copolymers with two different PTMO molecular weights (ca. 1000 and 2000 g/mol) are studied. The HS of these polyureas were based on *single* molecules of either 1,6-hexamethylene diisocyanate (HDI), 1,4-phenylene diisocyanate (*p*PDI) or 1,4-*trans*-cyclohexyl diisocyanate (CHDI). The SS molecular weight effects on the structure–property relationships for all the segmented polyureas were analyzed with DMA, tensile tests, SAXS and atomic force microscopy (AFM). The melt rheology and thermal stability of the HDI polyureas are also presented relative to ESTANE® 5750, a commercially available polyester-based TPU.

2. Experimental

2.1. Materials

1,4-Phenylene diisocyanate (*p*PDI) was purchased from Aldrich. *trans*-1,4-Cyclohexyl diisocyanate (CHDI) was purchased from DuPont. 1,6-Hexamethylene diisocyanate (HDI) and toluene diisocyanate (TDI) were kindly provided by Bayer. All diisocyanates, except *p*PDI were used as received, while *p*PDI was sublimed at 70 °C. Purities of diisocyanates were better than 99.5%. α,ω-Aminopropyl terminated poly(tetramethylene oxide) (PTMO-NH_2-1K) with $\langle M_n \rangle$ of 1100 g/mol was purchased from Aldrich. Poly(tetramethylene oxide)-glycol (PTMO-OH-2K) with $\langle M_n \rangle$ of 2050 g/mol was kindly provided by DuPont. α,ω-Aminopropyl terminated poly(tetramethylene oxide) (PTMO-NH_2-2K) with $\langle M_n \rangle$ of 2450 g/mol was prepared in our laboratories using the procedure described below. Borane–tetrahydrofuran complex (1 M), 15-crown-5 (98%), reagent grade acrylonitrile, tetrahydrofuran (THF), dimethylformamide (DMF) and isopropyl alcohol (IPA) were

purchased from Aldrich. THF was dried over molecular sieves and fractionally distilled. Other solvents were used as received. Sodium hydride suspension (60% in paraffin oil) was obtained from Merck ESTANE 5750 was kindly provided by Noveon.

2.2. Synthesis of α,ω-aminopropyl terminated PTMO (PTMO-NH_2-2K)

Amine-terminated PTMO (PTMO-NH_2-2K) was prepared in two steps, by the reaction of PTMO-OH-2K with excess acrylonitrile, followed by the hydrogenation of the nitrile groups to amine functionalities, using borane–tetrahydrofuran complex [15] (Scheme 1).

Reactions were carried out in a three-neck round bottom flask fitted with an overhead stirrer, nitrogen inlet and addition funnel. In the first step, 10.25 g PTMO-OH-2K, 20 mg 15-crown-5 were dissolved in 13.25 g acrylonitrile and cooled in an ice-water bath. Sodium hydride (5 mg) was added and the mixture was stirred for 15 min. The reaction was terminated by the addition of one drop of concentrated hydrochloric acid. Acrylonitrile was removed in a Rotavap, followed by vacuum drying (yield 89.3%). Bis(2-cyanoethyl) terminated poly(tetramethylene oxide) (PTMO-CN-2K) obtained was characterized by FTIR and ^{1}H NMR. In the second step 9.00 g PTMO-CN-2K was dissolved in 20 mL of dry THF and slowly added into the reactor containing 40 mL of 1 M borane–tetrahydrofuran complex in an ice-water bath. The solution was stirred for 30 min at 0 °C, followed by a reflux for 4 h. After cooling in an ice-water bath, 40 mL methanol was added dropwise, followed by the addition of 2 mL concentrated hydrochloric acid. The reaction mixture was stirred for 1 h. Solvent was removed under reduced pressure. To regenerate the amine end groups the product was treated with 50 mL of 1 M aqueous sodium hydroxide solution. The PTMO-NH_2-2K thus produced was extracted with methylene chloride and dried under vacuum (yield 86.6%). End group titration with standard HCl gave a number average molecular weight of 2450 g/mol for PTMO-NH_2-2K.

2.3. Polymer synthesis

Polymerizations were also conducted in three-neck, round bottom, Pyrex reaction flasks equipped with an overhead stirrer, addition funnel and nitrogen inlet. All copolymers were prepared by reacting equimolar amounts of a selected diisocyanate and PTMO oligomer. No chain-extenders were utilized. Polymerization reactions were carried out at room temperature in DMF (at a concentration of about 15–20% solids) by the dropwise addition of PTMO solution onto the diisocyanate solution under strong agitation. Completion of the reactions was determined by monitoring the disappearance of the isocyanate absorption peak around 2270 cm^{-1} with an FTIR spectrophotometer.

2.4. Film preparation

Polymer films with thicknesses of 0.5–1 mm were obtained by pouring the solutions into Teflon molds. The molds were covered with a glass Petri dish to slow down the solvent evaporation and placed in an oven maintained at 60 °C. After evaporation of the solvent, the molds were placed in a vacuum oven at 60 °C for complete drying, which was monitored gravimetrically. The resulting films were then removed from the Teflon molds and stored under vacuum at room temperature until needed for testing. The air side of the films (i.e. the side not touching the Teflon mold) was used for tapping-mode AFM analysis. Films of ESTANE 5750 used for melt rheology were prepared by compression molding, beads of the TPU in a PHI compression molder. Dried ESTANE beads were placed in a square mold and compressed at 170 °C and 20 psi pressure for 2 min. The molten sample were vented twice during the compression molding to allow degassing. The molded films were stored under dry conditions until tested.

2.5. Characterization methods

2.5.1. Dynamic mechanical analysis (DMA)

A Seiko DMS 210 tensile module with an attached autocooler for precise temperature control was used in tension mode. Rectangular samples (16 mm × 0.2–0.3 mm) were cut from cast films. Dynamic mechanical spectra of samples were recorded (at a heating rate of 2 °C/min), while they were deformed (10 μm amplitude, 1 Hz frequency) in the tension mode, under a nitrogen atmosphere.

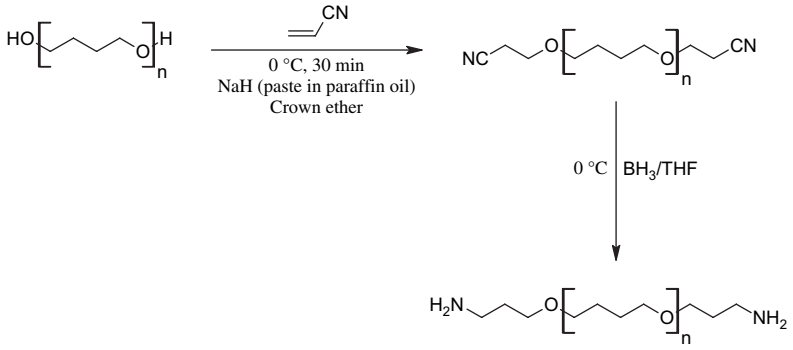

Scheme 1. Reaction scheme showing the preparation of amine-terminated 2K-PTMO.

2.5.2. Modulated differential scanning calorimetry (mDSC)

A TA Instrument Q100 DSC with refrigerated cooling system was used. Samples (2–4 mg) were enclosed in aluminum hermetic pans. Samples were cooled to −90 °C, equilibrated for 15 min and then heated to 150 °C at 2.5 °C/min, with a temperature modulation of 1 °C for every 60 s.

2.5.3. Tensile testing

An Instron model 4400 Universal Testing system controlled by Series IX software was used. A bench-top die was used to cut dog-bone-shaped samples (10 mm × 2.91 mm) from cast films. Samples were deformed until failure at a cross-head speed of 25 mm/min at room temperature.

The ambient temperature hysteresis behavior was recorded with dog-bone-shaped samples having similar dimensions as described above. Samples were stretched to 300% strain (25 mm/min cross-head speed) and then brought back to its initial 0% strain conditions, at the same cross-head speed. Each sample was subjected to four loading–unloading cycles.

Stress–relaxation experiments were also conducted (sample dimension: 15 mm × 0.3–0.35 mm) at room temperature. Samples were loaded (10 mm/min cross-head speed) to 10% strain and the stress decay was measured for 3 h.

2.5.4. Tapping-mode atomic force microscopy (AFM)

Phase images of the segmented copolymer samples were captured at ambient conditions using a Veeco atomic force microscope equipped with a Nanoscope IVa controller. Nanosensors™ Point Probe® Plus non-contact/tapping mode, high resonance frequency with a reflective aluminum coating (PPP-NCH-50) was used for imaging. These tips had a nominal force constant of 42 N/m, resonance frequency of ~320 kHz and a radius of curvature <10 nm. Images were captured at 1 Hz frequency and a set-point ratio of ~0.6 (medium to hard tapping) at ambient conditions.

2.5.5. Melt rheology

A TA Instrument AR-G2 rheometer fitted with 8 mm stainless steel parallel plates was used. Sample discs of 8 mm were cut from cast film with a circular die. All experiments were conducted at 170 °C. Sample discs were loaded in-between the parallel plates (1000 μm gap) and were initially subjected to a strain sweep (0.01–10% strain at 1 Hz frequency). All samples were found to be within their linear viscoelastic region in the applied strain limits. The same sample was then subjected to three frequency sweeps (0.1–10 Hz) at 1% strain.

2.5.6. Small-angle X-ray scattering (SAXS)

Data were collected at the Army Research Laboratory using a 3 m SAXS camera with pinhole collimation and a molecular metrology multi-wire area detector. Cu-Kα X-rays are generated using a Rigaku Ultrax18 rotating at 40 kV and 115 mA, and are filtered with nickel foil to give a wavelength (λ) of 1.5418 Å. The samples were characterized at a sample-to-detector distance of approximately 150 cm. Beam center and camera length are routinely calibrated using a silver behenate standard. The raw data are corrected for background noise and transmission prior to azimuthal averaging, and the corrected data are scaled to absolute intensity using data from a sample of type 2 glassy carbon which was previously calibrated at the Advanced Photon Source, Argonne National Laboratory, Argonne, IL. All data reduction and averaging were done using Wavemetrics' IGOR Pro v. 5.04B, and procedures written by Dr. Jan Ilavsky of Argonne National Laboratory. The SAXS data are presented as intensity, I, versus scattering angle, s, where $s = 2 \sin \theta/\lambda$, where 2θ is the radial scattering angle.

3. Results and discussion

Previous reports [16–20] from our laboratory have shown that most non-chain extended, segmented polyureas based on PTMO SS of molecular weight 1100 g/mol, display a percolated hard microphase separated morphology even at a relatively low HS content (~13%). They also display a distinctly broader service temperature window and soften at higher temperatures compared to the corresponding urethane analogues. This difference is attributed to bidentate hydrogen bonding between urea linkages which is more cohesive than the monodentate hydrogen bonding between the urethane linkages [16,18–20]. Limited compression molding data showed that some of the polyureas and polyurethanes were moldable from their melt states [16]. In the present study, the molecular weight of the PTMO SS was increased from 1100 to 2450 g/mol, which in turn reduced the HS contents of the resultant polyureas dramatically (by ca. 50%). In this study, the polyureas based on 1100 and 2450 g/mol PTMO SS will be designated as 1K and 2K polyureas. The HS contents of the different polyureas under investigation were measured from solution proton NMR and are shown in Table 1. As mentioned earlier, most 1K-polyureas showed a microphase separated structure, where the HS formed thread-like structures that percolated throughout the SS continuous matrix [16,18].

Our goal in this study is to investigate the effect of the SS molecular weight on the mechanical and melt rheological properties of the polyureas, and whether they are still able to form a percolated hard microphase morphology, at the lower HS content (ca. 6 wt%).

3.1. Thermal analysis

The dynamic mechanical responses of non-chain extended, segmented polyureas, with the HS based on single molecules of HDI, CHDI or *p*PDI and the SS based on PTMO with

Table 1
HS contents of the non-chain extended, segmented polyureas investigated

Amine-terminated PTMO molecular weight (g/mol)	HS content of polyurea based on different diisocyanates (wt%)		
	HDI	CHDI	*p*PDI
1100	13.3	13.1	12.7
2450	6.3	5.7	5.5

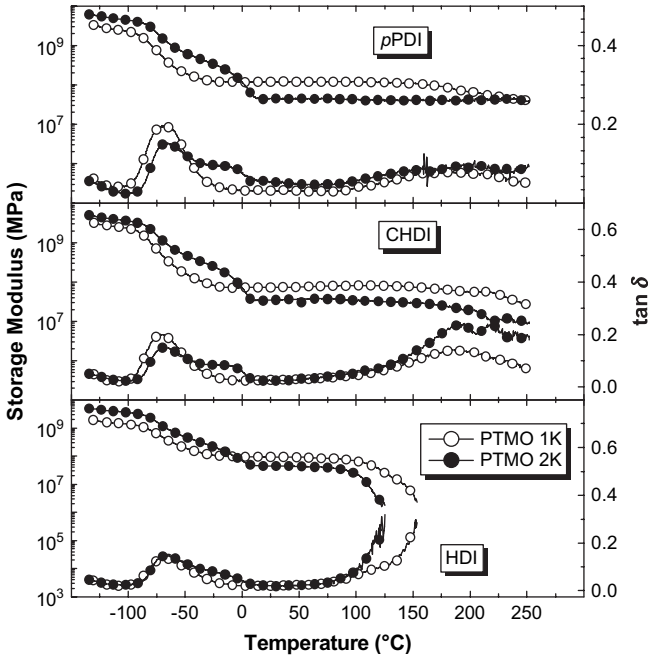

Fig. 1. Effect of PTMO SS molecular weight and diisocyanate type on the dynamic mechanical spectra of non-chain extended, segmented polyureas.

two different molecular weights (ca. 1K and 2K g/mol) are shown in Fig. 1. At very low temperatures (−130 to −100 °C), the modulus of the 2K-polyureas was found to be consistently higher than the corresponding 1K-polyureas in all cases, which is believed to be due to the greater presence of PTMO SS crystallites in the 2K-systems which will be addressed later. In all polyureas, the onset of T_g of the PTMO SS occurred in the storage modulus, E', at ca. −90 °C (which led to a decrease in E'; ca. 1 decade for 1K polyureas and ca. 2 decades for the corresponding 2K polyureas) and the corresponding tan δ displayed a peak centered at ca. −60 °C. The tan δ peaks of all the 2K-polyureas also showed a distinct shoulder, which was barely apparent in the corresponding 1K analogues. This shoulder is due to the melting of the partially crystalline PTMO SS, which occurs at low temperatures. (This issue will be addressed later in this report using DSC data analysis of the materials.) This was followed by a rubbery plateau region, with a modulus of $\sim 1 \times 10^8$ for the 1K polyureas and $\sim 4 \times 10^7$ Pa for the corresponding 2K polyureas.

Similar effects of SS molecular weights on the plateau modulus of siloxane–urea segmented copolymers were reported previously [8]. Such high rubbery plateau moduli are only commonly exhibited by conventional chain extended polyurethanes with much higher HS content than those observed in our copolymers (ca. ~13 wt% for 1K and ~6 wt% for 2K polyureas). The breadth of the rubbery plateau and the inception of an upper softening point were found to greatly depend on the nature, symmetry and "stiffness" of the diisocyanates. HDI based aliphatic polyureas, which contain only methyl groups between the urea linkages, softened at ca. 100 °C (1K), while the incorporation of either the 1,4-*trans* cyclic moieties (cyclohexane ring) for CHDI or an aromatic phenyl ring for *p*PDI, between the urea linkages of the HS, resulted in significant increases in the upper softening point temperatures. The molecular weight of the PTMO SS also had distinct effects on the polyurea service windows. With an increase in the SS molecular weight, while the inception of the rubbery plateau shifted to higher temperatures (which is due to melting of PTMO SS crystallites; see discussion below), the rubbery/viscous flow was observed to occur at a lower temperature relative to the 1K polyurea.

The distinct effects observed due to the increase in the PTMO SS molecular weights on the DMA scans of different polyureas (higher modulus at low temperature and a tan δ shoulder at ca. −10 °C) are due to the increase in the SS crystallinity. It is known that PTMO SS may crystallize at low temperatures if the SS molecular weight is sufficient and if the kinetics of crystallization is favorable. But an increase in the SS molecular weight also leads to generation of greater amount of SS crystallites and elevation of the SS crystal melting temperature [21]. The crystallinity of both the SS and the HS of our polyureas was thus characterized by DSC and is illustrated in Fig. 2 for the HDI based polyureas.

Both polyurea copolymers showed an endothermic transition at ca. −70 °C, due to the T_g of the PTMO SS. While, the 1K polyurea showed a small endothermic peak at ca. −25 °C, a distinctly larger endothermic melting peak was observed at ca. 0 °C for the 2K polyurea. This larger peak also led to a distinctly higher heat of fusion arising from the SS crystallites in the 2K polyurea relative to its 1K analogue. Similar observations were also noted for the analogous CHDI- and *p*PDI-polyureas. Both the 1K and 2K polyureas also displayed a high temperature endothermic peak due to the melting of the HS crystallites; but the HS melting occurred at a lower temperature (103 °C) in the 2K polyureas relative to the corresponding 1K analogue (116 °C) – the reader please recall that the viscous flow in the DMA profiles of the 2K polyureas (Fig. 1) also started at a lower temperature relative to the corresponding 1K polyurea. This decrease in HS melting temperature may be due to the lower perfection of the HS crystals

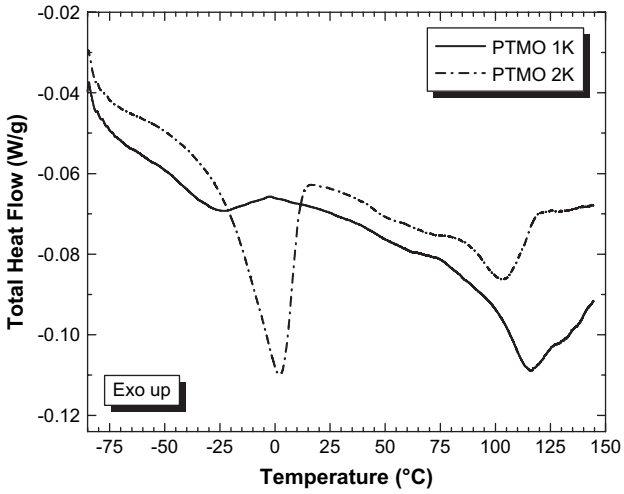

Fig. 2. Effect of PTMO SS molecular weight on the mDSC profiles of non-chain extended, segmented polyureas based on HDI HS.

caused by the much lower weight fraction in the 2K system but the morphological analysis of these systems by AFM (presented later) does not strongly support this conjecture. Another postulation for the decrease in HS melting temperature with increase in SS molecular weight may extend from rubber elasticity theory. An increase in SS molecular weight may potentially increase the severity of SS chain motions with rising temperatures in the rubbery plateau service windows of these polymers (which is above the SS T_g), which in turn increases the effective stress on the HS crystals (which are linked covalently to the SS), thereby driving the HS melting point down. Integration of the high temperature melting endotherms showed that the heat of fusion for the HS melting was almost double for the 1K polyurea relative to the corresponding 2K polyurea. This may not be surprising because the HS content was almost double in the 1K polyureas (recall Table 1). However, it is noteworthy that these results strongly support the fact that even with only ca. 6 wt% HS, these single molecular HS residues can still form a distinct crystalline phase.

3.2. Morphological analysis by tapping-mode AFM

Relatively high modulus of the rubbery plateau (Fig. 1) in 1K and 2K polyureas both possessing low HS contents implies the presence of considerable percolation/connectivity of the HS phase throughout the dominant SS matrix. This was verified by performing tapping-mode AFM characterization (which is a surface characterization technique) on the top surface of the solution-cast polyurea films and is shown in Fig. 3 with polyureas based on HDI and *p*PDI hard segments.

Both the 1K polyureas (Fig. 3A and C) displayed thread-like crystalline hard domains of high aspect ratio, which appear from the AFM phase images to be well connected throughout the SS continuous phase. These ribbon-like hard domains are formed by the crystallization of the symmetric *p*PDI and HDI hard phases [confirmed by DSC (Fig. 2) and WAXS (1K polyureas)], which in turn results in the high rubbery plateau modulus, even with such low HS contents (ca. 13 wt%). The AFM phase images of the corresponding 2K polyureas (Fig. 3B and D) show that even with ca. 6 wt% HS, they were able to phase separate to form a similar thread-like crystalline HS morphology.

While the thread-like HS structures seem to be of the same size in both 1K and 2K analogues, the density of the hard domains appears to be distinctly higher in the 1K polyureas, relative to the corresponding 2K analogues; as might be expected due to their low volume/weight fraction relative to their 1K analogues. The AFM phase images may suggest that all

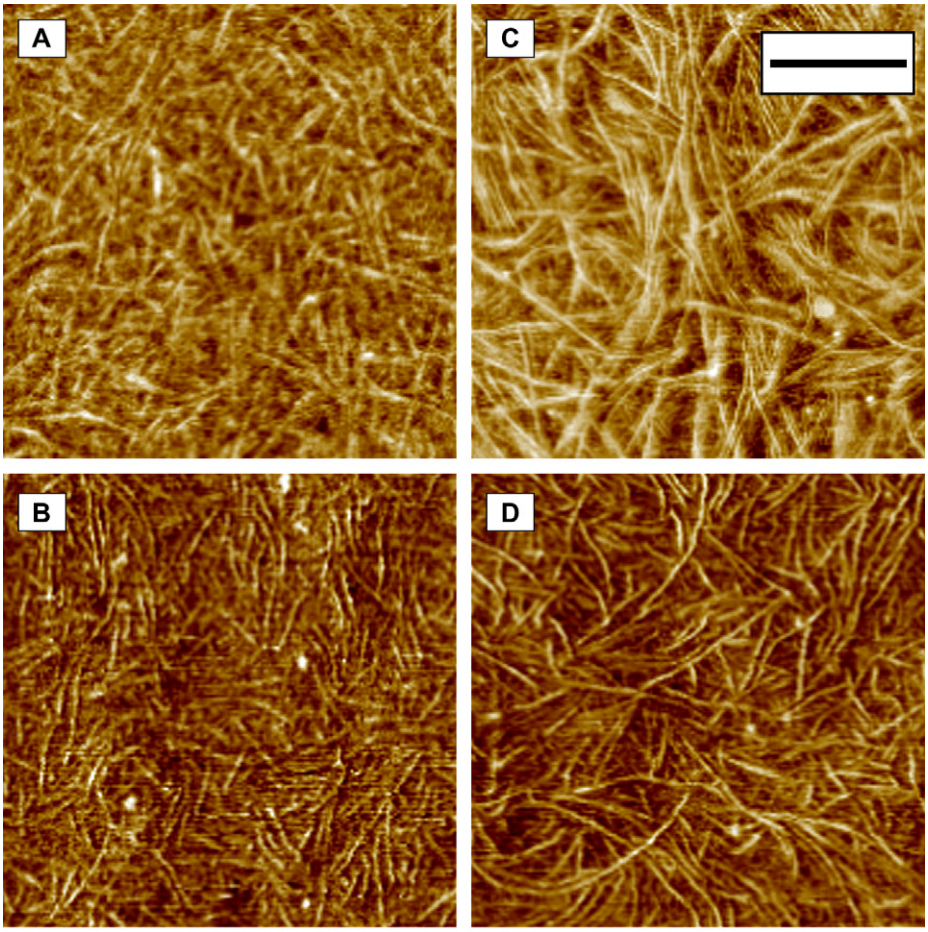

Fig. 3. Tapping-mode AFM phase images of selected non-extended, segmented polyureas: (A) PTMO(1K)-*p*PDI, (B) PTMO(2K)-*p*PDI, (C) PTMO(1K)-HDI, (D) PTMO(2K)-HDI. The bar denotes 200 nm.

the polyureas possess a percolated morphology, but conclusive proof for the percolation of the HS phase through the SS matrix could not be garnered from the AFM images. This is due to the fact that the medium-to-hard tapping (set-point ratio = 0.6) employed in obtaining the AFM phase images, leads to the contribution of several underlying layers to the observed patterns. Additional evidence about the presence of a percolated phase separated structure could be obtained if these polyureas displayed distinct necking/yield point (which arise due to the breakdown of percolated hard phase), when stretched uniaxially. These results will be presented shortly. It should also be pointed out that a similar microphase morphology was also obtained for the CHDI-polyureas, which is not shown here.

3.3. SAXS analysis

Further verification of the microphase separated structures of these single hard segment polyureas was also obtained by analyzing the SAXS profiles of the polyureas, which unlike AFM, is a bulk characterization technique. This is shown in Fig. 4 for the 1K and 2K HDI polyureas. Both polyureas showed a first order scattering peak in their respective intensity profiles indicating the presence of a microphase separated morphology at ambient conditions. The position of the interference peak in the respective scattering intensity profile was used to estimate the Bragg or d spacing ($\sim s_{max}^{-1}$) in the sample, which may be interpreted as an average interdomain spacing arising from the presence of periodic structure (on a short-range scale length). As expected, the average interdomain spacing was found to increase with the PTMO SS molecular weight; the longer PTMO-2K chains gave rise to a higher d spacing (103 Å) relative to the corresponding 1K analogue (79 Å). Similar results were also obtained for the *p*PDI based polyureas, where increase in the PTMO SS molecular weight led to an increase in the interdomain spacing of the HS. SAXS analysis of the CHDI-polyureas was not performed.

3.4. Tensile testing

The stress–strain behavior was next analyzed in order to note the extent of hard phase connectivity and mechanical performance of the polyureas with respect to elongation at break and ultimate tensile strength. When stretched uniaxially at ambient conditions, systems with a long-range HS connectivity and a well percolated hard phase throughout the soft matrix display a yield point, due to the breakup of the percolated hard phase. Fig. 5 compares the tensile behavior of 1K and 2K polyurea based on HDI hard segments.

Results showed that only the 1K polyurea had a distinct yield point at room temperature. Now it is a well-known fact that when stretched uniaxially at ambient conditions, systems with a long-range HS connectivity and a well percolated hard phase throughout the soft matrix display a yield point, due to the breakup of the percolated hard phase [2,4,16,18,22]. This led us to postulate that though both the polyureas display morphology with apparent HS percolation as noted by AFM phase images (Fig. 4), the long-range HS connectivity may only be truly present in the 1K polyurea systems, which possess twice the HS content relative to their corresponding 2K systems. Interestingly, the increase in PTMO molecular weight had little effect on the ultimate tensile strength and elongation to break for both of these systems. It is surprising to note that even with only ca. 6 wt% HS content, the 2K polyurea had a tensile strength (~30 MPa) and elongation at break (~1000%) comparable to or often exceeding many of the commercial chain extended TPEs with significantly higher HS contents. Similar results were also obtained for polyureas based on *p*PDI and CHDI hard segments (i.e. while only the 1K systems showed a distinct yield point, both systems had comparable ultimate tensile strength and elongation at break values).

Fig. 6 and Table 2 illustrate the effect of PTMO SS molecular weight on the mechanical hysteresis (MH) of all three of the 1K and 2K segmented polyureas, which were made to undergo four deformation cycles (but only the first two cycles are shown in this study).

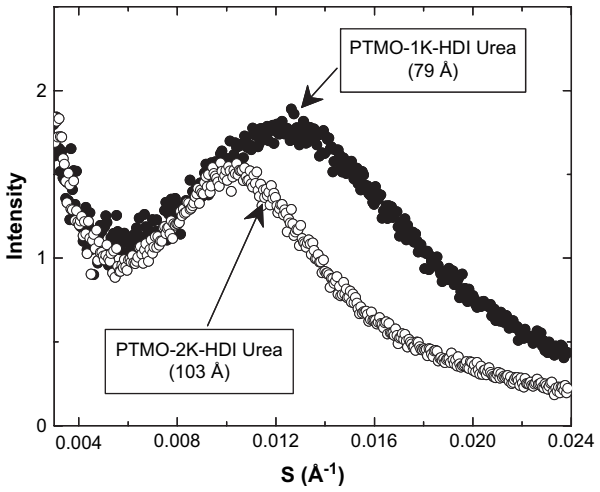

Fig. 4. Effect of PTMO SS molecular weights on the SAXS profiles of non-chain extended, segmented polyureas based on HDI HS.

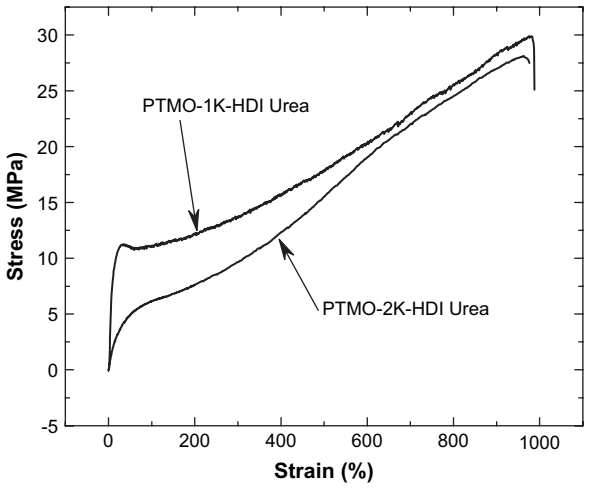

Fig. 5. Effect of PTMO SS molecular weight on the tensile curves of non-chain extended, segmented polyureas based on HDI.

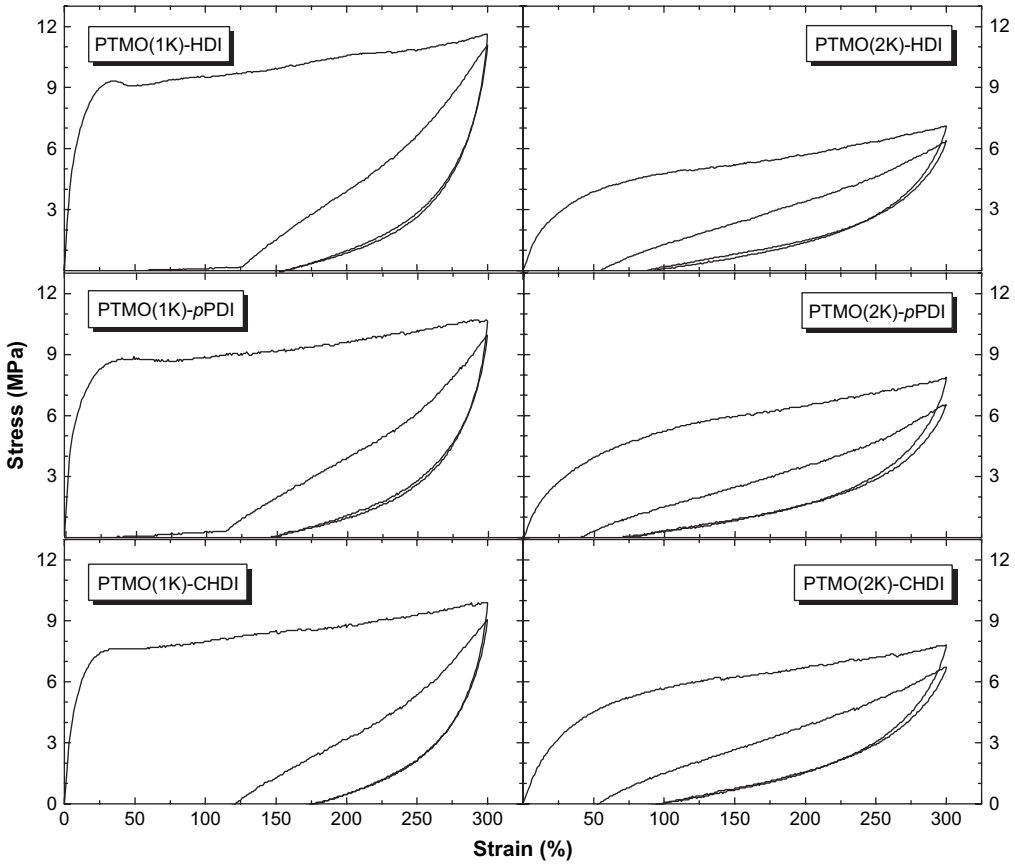

Fig. 6. Effect of PTMO SS molecular weight on the hysteresis behavior (first two cycles) of non-chain extended, segmented polyureas based on HDI HS.

In the first deformation cycle, as the polyureas were elongated to 300% strain followed by withdrawal of the applied load, significant MH was observed, due to the breakup and restructuring of the hard phase. A distinct yield point was also observed for all the 1K polyurea systems. The following deformation cycle led to significantly lower MH values in all polyureas analyzed. This may be attributed to the fact that the percolated hard segments which were broken in the first deformation cycle did not have time to reheal; thus the load was sustained by the continuous soft matrix which in turn gave rise to greater elasticity and lower MH.

As expected, the MH was found to decrease with an increase in the PTMO SS molecular weight in both cycles. This also indirectly points to the decrease in the hard phase connectivity in the polyureas with increase in SS molecular weight. The subsequent third and fourth deformation cycles (not shown) were found to be similar to the second deformation cycle (with similar mechanical hysteresis values) for all the polyureas tested. The specific diisocyanate used for the hard segment was found to have little effect on the hysteresis behavior of the polyureas analyzed. Significant permanent set (Table 2) was observed for the 1K polyureas, which decreased substantially with the increase in the PTMO SS molecular weights.

Table 2
Mechanical hysteresis and permanent set values of the segmented, non-chain extended polyureas with different PTMO SS molecular weights

Polyurea HS	PTMO SS molecular weights (g/mol)	Mechanical hysteresis (MH) (%)		Instantaneous permanent set after first cycle (%)
		Cycle 1	Cycle 2	
HDI	1100	88	56	156
	2450	75	48	90
*p*PDI	1100	87	56	150
	2450	74	47	75
CHDI	1100	89	60	177
	2450	76	51	100

3.5. Effect of deformation on polyurea morphology

The effect of stress on the morphology of these segmented, non-chain extended polyureas based on HDI HS and 1K PTMO SS was investigated with tapping-mode AFM and is shown in Fig. 7. Fig. 7A shows the phase image of the unoriented polyurea, where the thread-like HS microphases were randomly distributed in the continuous SS matrix. Fig. 7B shows the phase image of the polyurea, uniaxially stretched to 150% (stretch direction is shown by arrow), which was beyond the yield point of the sample (recall Fig. 5). Upon deformation, the HSs were found to break into distinctly smaller and less defined, thread-like structures which oriented along the stretch direction, similar to the behavior of other segmented copolymers, which possessed morphology similar to our systems [13,14], except our HS which comprises only

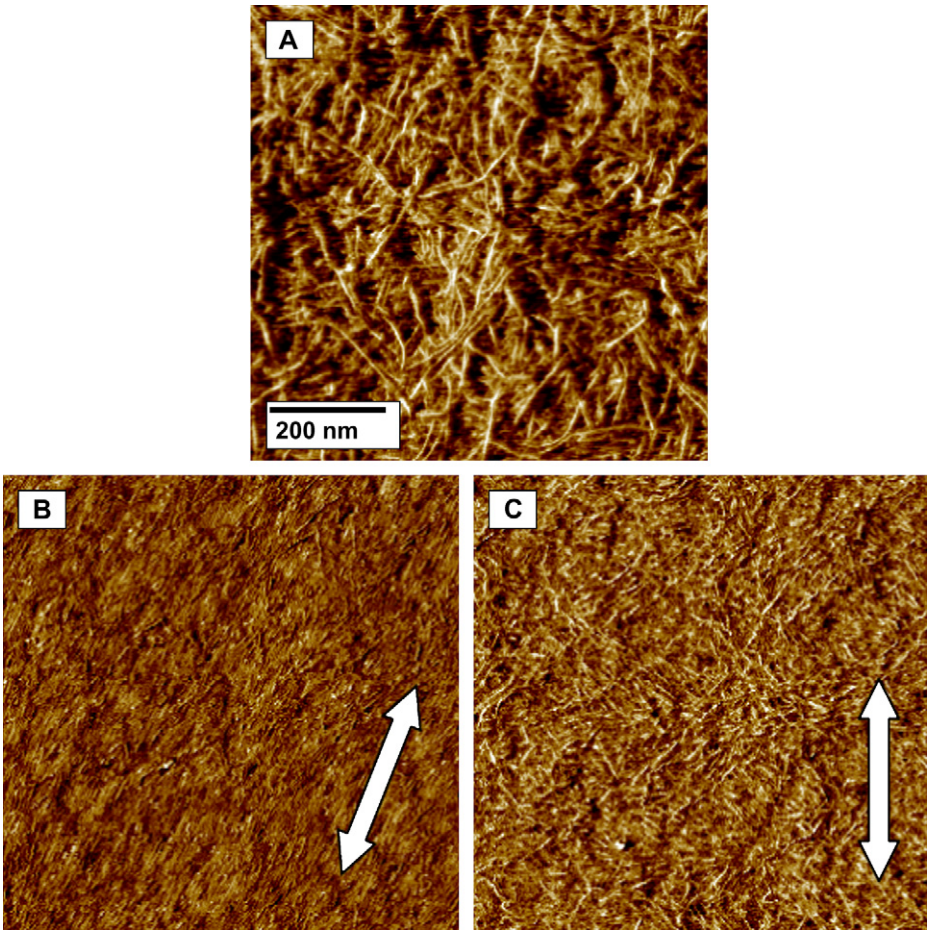

Fig. 7. Ambient tapping-mode AFM images of PTMO-1K-HDI polyurea under various conditions: (A) undeformed, (B) uniaxially stretched to 150% (image obtained within 2 h of stretch), (C) uniaxially stretched to 150% and relaxed without stress for 24 h (stretch direction is shown by arrow).

one molecule (diisocyanate). In order to examine if the stretched sample regained its initial undeformed morphology on removal of the stress, a sample was deformed uniaxially to 150% strain, allowed to relax without stress for 24 h and its phase image was recorded (Fig. 7C, the original stretch direction is shown by the arrow). The segmented polyurea was found to form a similar microphase separated morphology with randomly oriented thread-like HS crystals, which, however, were distinctly shorter than those observed in the undeformed sample.

The AFM phase image of the stretched and relaxed sample (Fig. 7C) illustrates that after deformation, the sample partially regains its original morphology but the extent of the HS connectivity in the sample could not be easily judged from the AFM phase image, due to reasons stated earlier. In order to investigate if the polyureas still possessed the percolated microphase separated morphology, the tensile behavior of the 1K polyurea was tested before and 24 h after it had undergone 300% deformation, which is shown in Fig. 8. The polyurea was initially stretched to 300% deformation (cycle 1), after which the load was removed and the sample was allowed to relax for 24 h. The permanent set of the polyurea samples at that time was 120%. Taking this as the initial length, the sample was further deformed to 150% deformation (see Fig. 8, cycle 2). As can be seen in Fig. 8, yield points were observed for the polyurea samples in cycle 1, but when the samples were deformed again (after being allowed to relax without load for 24 h), a yield point was not observed (cycle 2). This illustrates that the deformed samples after relaxation

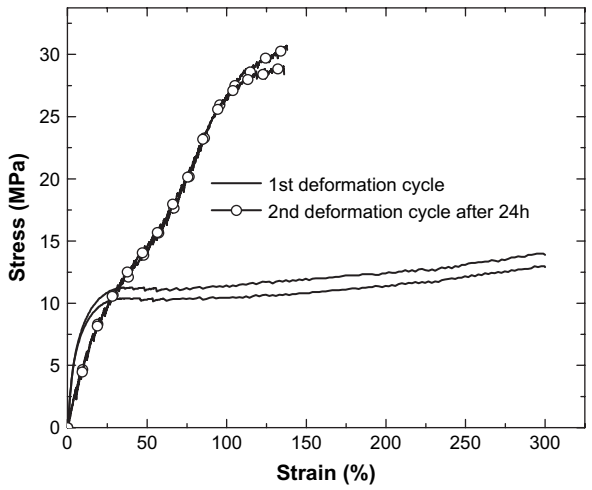

Fig. 8. Stress–strain curves of 1K polyurea based on HDI before and after 300% deformation (two replications each).

for 24 h partially heal to their original microphase separated morphology but full connectivity of the HS thread-like domains may not occur. Similar behavior was also observed for the *p*PDI- and CHDI-based 1K PTMO polyureas. The modulus of the samples (determined from the slope of the linear part of the stress–strain curve) was also observed to decrease from cycle 1 to cycle 2. The stress on the sample at 150% strain was found to increase (from ca. 12 to 30 MPa) from cycle 1 to cycle 2. This may be due to strain-induced crystallization of the PTMO SS and which will be addressed along with a more complete description of the effects of deformation on the morphology of these segmented, non-chain extended polyureas as well as polyurethanes, in a future paper utilizing real time SAXS and WAXS analyses [23].

3.6. Stress–relaxation behavior

The effect of altering the PTMO SS molecular weights on the stress–relaxation behavior of the polyureas was analyzed by applying an instantaneous, constant strain of 10%, which was below the yield points (for 1K polyureas) of stress–strain curves of all polyureas, followed by measuring the stress decay with time at ambient conditions. Fig. 9A shows two replications of the decay of absolute stress with time for segmented, non-chain extended polyureas based on HDI and PTMO with different molecular weights. A twofold increase in SS molecular weight led to a decrease in the stress-level by a factor of almost four. In Fig. 9B, each curve (from Fig. 9A) was normalized by their initial stress, generating curves which show the time-dependent stress decay (or rate of stress decay) of the polyureas. With the increase in the SS molecular weight (and therefore lower HS weight fractions), the rate of stress decay was found to increase as might well be expected.

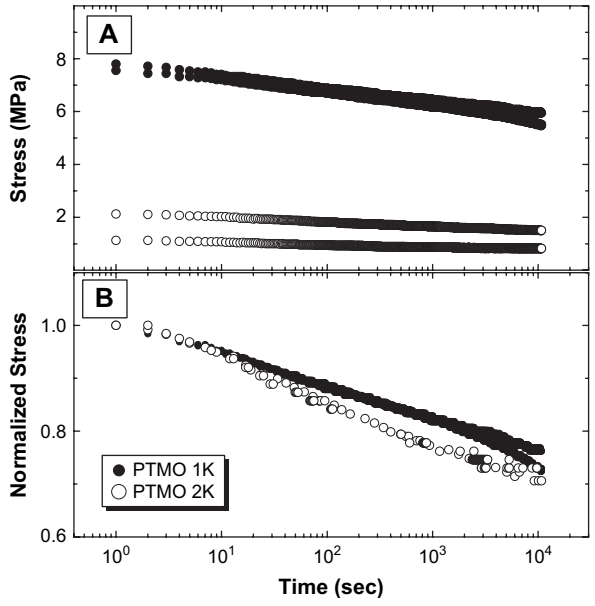

Fig. 9. Effect of PTMO SS molecular weight on the stress–relaxation behavior of non-chain extended, segmented polyureas based on HDI HS (two replications each).

3.7. Prediction of ambient tensile modulus

Utilizing all the results presented so far, it was concluded that all the 1K PTMO based segmented polyureas based on a single diisocyanate molecule as the HS, exhibit a microphase separated morphology, where the HS domains form ribbon-like crystalline structures of high aspect ratio that percolated throughout the continuous SS matrix. These thread-like hard domains thus act as both a reversible pseudo-crosslink and reinforcing filler in the soft PTMO matrix. Thus, the hard domains may also be viewed as randomly dispersed fibers, reinforcing the continuous matrix in a fiber-reinforced composite. With this morphological view in mind, as a zeroth approximation, we utilized a composite model for predicting the observed tensile modulus. The model we selected was proposed by Christensen [24], which has been commonly used to model fiber-reinforced composites where the fibers are oriented randomly in both two- (2D) and three-dimension (3D), and is shown below (model only applicable for systems with $v_f < 0.2$).

Christensen 2D random:

$$E_c = \frac{v_f}{3}E_f + \left(1 + v_f\right)E_m \tag{1}$$

Christensen 3D random:

$$E_c = \frac{v_f}{6}E_f + \left[1 + \left(1 + v_f\right)\right]E_m \tag{2}$$

where, E_c is the predicted modulus, E_f is the fiber modulus, E_m is the matrix modulus, and v_f is the fiber volume fraction.

Previously, this model in conjunction with two others has been used for correctly predicting the tensile modulus of segmented polyurethanes based on a single *p*PDI HS and soft segment based on 1000 g/mol PTMO [17]. Generally, the tensile modulus of a highly unoriented, semicrystalline polymer below its T_g and a rubbery polymer ranges between $1-10 \times 10^9$ and $1-10 \times 10^5$ Pa, respectively. Thus for our calculation, we assumed E_f to be 5×10^9 Pa and E_m to be 5×10^5 Pa. We also assumed that the densities of the HS and SS in the copolymer were similar to their corresponding precursors (PTMO for SS and diisocyanate for HS), which allowed us to convert the HS weight fractions (w_f) to volume fractions by using the densities of the PTMO (ρ_{SS}) and the diisocyanate (ρ_{HS}) (Eq. (3)).

$$v_f = \frac{w_f \rho_{HS}}{\left(100 - w_f\right)\rho_{SS} + w_f \rho_{HS}} \tag{3}$$

Using Eq. (3) for the polyurea based on *p*PDI hard segments, the v_f of PTMO(1K) polyurea (13 wt% HS) was 0.11 and that for PTMO(2K) (5.5 wt% HS) was 0.05, while that of PTMO-1K-HDI and PTMO-2K-HDI polyureas were 0.12 and 0.06, respectively [note: this assumes that all the HS are in the crystalline form]. Table 3 shows the tensile modulus of *p*PDI and HDI polyureas predicted by the Christensen model and that obtained from DMA at ambient conditions.

Table 3
Comparison of the tensile modulus values predicted by Christensen model to that of the experimental modulus obtained from DMA at 23 °C

Polyurea	Modulus predicted by Christensen model (Pa)		Modulus measured by DMA (Pa)
	2D random	3D random	
PTMO(1K)-*p*PDI	1.86×10^8	9.40×10^7	1.18×10^8
PTMO(2K)-*p*PDI	7.80×10^8	3.98×10^7	4.47×10^7
PTMO(1K)-HDI	2.04×10^8	1.03×10^8	9.39×10^7
PTMO(2K)-HDI	9.38×10^7	4.76×10^7	4.78×10^7

The experimental modulus values were observed to match closely with the Christensen composite model for a composite with 3D random fiber orientation. This close agreement between the predicted and experimental modulus values was somewhat surprising in view of the fact that the model is valid for composites reinforced with *short fibers* and in the *absence of any chemical bonds* between the fiber and the matrix. But in our systems, the HS segment threads are of high aspect ratio and in addition there are covalent linkages between the HS and the continuous SS. In spite of these limitations, the Christensen model provided a close prediction between the calculated and experimental tensile modulus, which confirmed our hypothesis that the ribbon-like HS domains act as reinforcing fillers for the soft, continuous PTMO matrix.

3.8. Melt rheology

As mentioned earlier, most of the commercially available thermoplastic segmented copolymers (TPEs) are either polyurethane, poly(ether-*block*-ester) or poly(ether-*block*-amide) in nature. Segmented polyureas and even polyurethane–ureas (LYCRA®) are usually not melt-processible. As stated earlier, this is mainly due to: (i) very strong bidentate hydrogen bonding between urea groups and (ii) low thermal degradation temperatures of the urea linkages. In fact, high molecular weight urea hard segments containing several urea linkages, start degrading before they can be melt processed. Melt processible, segmented siloxane-based polyureas, which have chemical structures similar to those synthesized by Yilgor [6,7], have been recently commercialized. (Geniomer®, Wacker Chemie AG, Germany [25]). Colombani et al. [10] recently synthesized bis-urea grafted PDMS polymers, some of which were shown to be melt stable and processible at high temperatures. In another recent report, Versteegen et al. [14,15] synthesized segmented, copoly(ether urea)s with uniform hard segments, which were shown to possess excellent mechanical properties. They measured the flow temperatures (where materials lost their dimensional stability) of their block copoly(ether urea)s by optical microscopy. They noted as would be expected that the flow temperature was found to decrease with the soft segment length and increase with the number of urea groups in the hard segments [15]. Previously, we have also shown that some of the segmented, non-chain extended polyureas were moldable [16]. In the present study, we compared the melt rheology of the HDI HS based polyurea with a commercially

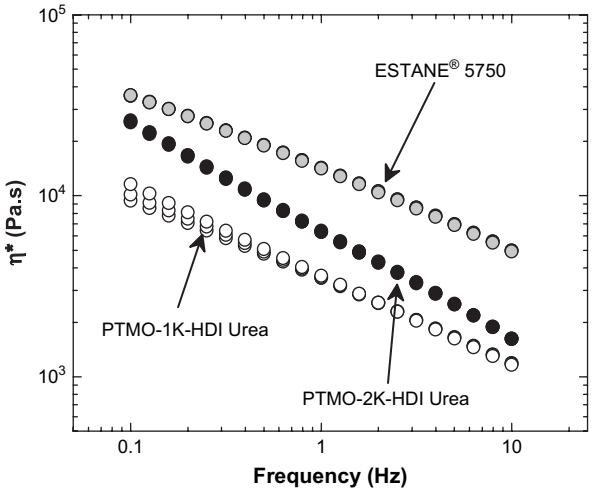

Fig. 10. Comparison of the melt rheology of commercially available TPE ESTANE® 5750 and non-chain extended, segmented polyureas based on PTMO SS and HDI HS at 170 °C.

available polyester-based TPE, ESTANE® 5750. The melt rheology of the other two polyureas (*p*PDI and CHDI) was not analyzed since they did not melt and still maintained a high modulus value even above 200 °C (recall Fig. 1). The melt rheology and melt stability of the copolymers were analyzed by performing multiple (three) frequency sweeps at 170 °C and observing the variation of the dynamic shear viscosity (η^*) of the polyureas with frequency (Fig. 10). Though, the above mentioned melt test temperature (170 °C) is somewhat lower than most commercial ESTANE® polyurethane processing temperatures, it was chosen because the DMA spectra of the polyureas showed the inception of flow behavior below that temperature, due to the melting of the HDI crystalline phase (recall Figs. 1 and 2).

As expected, all copolymers showed shear-thinning behavior. The melt viscosity of the segmented, non-chain extended polyureas was found to be lower than that of the commercial polyester-based TPE, but well within the conventional melt viscosity limits. With an increase in molecular weight of PTMO, the viscosity increased slightly. This may be attributed to different overall sample molecular weights which likely evolved in the synthesis of these polyureas. Though it is not evident, the above plot (Fig. 10) shows results from three consecutive frequency sweep experiments, where each copolymer was subjected to oscillatory shear forces (1% strain) for ca. 30 min at 170 °C. The dynamic viscosity versus frequency curves did not change with the frequency sweep cycles for the ESTANE copolymer, which was not surprising in view of the fact that this commercially available material is known to contain stabilizer additives.

But our copolymers, which did not contain any stabilizers also showed no (for 2K polyurea) or slight, but not significant (1K polyurea) viscosity changes with increasing frequency sweep cycles. This illustrates that our segmented, non-chain extended HDI based polyureas, containing low HS fractions are stable and should be melt-processible by conventional processing techniques like extrusion, injection molding, etc. The

addition of antioxidants and other conventional stabilizers would of course be expected to further improve the stabilization of these new, segmented polyureas to even higher melt processing temperatures.

4. Conclusions

The effect of soft segment (SS) molecular weight and diisocyanate structure on the structure–property relationships of novel, segmented, non-chain extended polyureas with hard segments (HS) based on a single diisocyanate molecule was investigated. These polyureas showed the presence of a microphase separated structure, with thread-like HS randomly dispersed throughout the SS matrix, even with very low, ca. 6 wt% HS contents. When deformed uniaxially beyond their yield point, the HS were found to breakup into smaller thread-like structures and orient themselves parallel to the stretch direction. Upon relaxation, the polyurea was shown to possess similar phase separated morphology. An increase in SS molecular weight led to increased formation of SS crystallites at low temperatures, which had a twofold effect: (1) it increased the tensile modulus of the polyureas at low temperatures and (2) adversely affected (shortened) the ''service window'' of the polyureas. The long-range HS connectivity, which was present in the 1K polyurea systems, was found to decrease with an increase in SS molecular weight, but both 1K and 2K analogues were found to possess similar mechanical properties (e.g. ultimate tensile strength and elongation at break). Both the 1K and 2K segmented, HDI based polyureas, were shown to be stable in the melt and melt processibility is expected.

Acknowledgements

This project was supported by the U.S. Army Research Laboratory and the U.S. Army Research Office under Grant No. (DAAD19-02-1-0275) Macromolecular Architecture for Performance (MAP) MURI.

References

[1] Legge NR, Holdenand G, Schroeder HE, editors. Thermoplastic elastomers: a comprehensive review. New York, NY: Hanser Publishers; 1987.
[2] Abouzahr S, Wilkes GL, Ophir Z. Polymer 1982;23:1077–86.
[3] Hepburn C. Polyurethane elastomers. New York, NY: Elsevier Applied Science Publishers; 1992.
[4] Abouzahr S, Wilkes GL. In: Folkes MJ, editor. Processing, structure and properties of block copolymers. London: Elsevier Applied Science Publishers; 1985. p. 165–207.
[5] Schollenberger CS. Handbook of elastomers. New York, NY: Marcel Dekker Inc; 2001.
[6] Yilgor I, Riffle JS, Wilkes GL, McGrath JE. Polymer Bulletin 1982;8: 535–42.
[7] Yilgor I, Shaaban AK, Steckle WP, Tyagi D, Wilkes GL, McGrath JE. Polymer 1984;25:1800–6.
[8] Tyagi D, McGrath JS, Wilkes GL. Polymer Engineering and Science 1986;26:1371–98.
[9] Tyagi D, Wilkes GL, Yilgor I, McGrath JS. Polymer Bulletin 1982;8: 543–50.
[10] Colombani O, Barioz C, Bouteiller L, Chaneac C, Formperieand L, Montes H. Macromolecules 2005;38:1752–9.
[11] Husken D, Krijgsmanand J, Gaymans RJ. Polymer 2004;45:4837–43.
[12] Niesten MCJE, Brinkeand JWT, Gaymans RJ. Polymer 2001;42:1461–9.
[13] Sauer BB, Mclean RS, Gaymans RJ, Niesten MCJE. Journal of Polymer Science, Part B: Polymer Physics 2004;42:1783–92.
[14] Versteegen RM, Kleppinger R, Sijbesmaand RP, Meijer EW. Macromolecules 2006;39:772–83.
[15] Versteegen RM, Sijbesmaand RP, Meijer EW. Macromolecules 2005;38: 3176–84.
[16] Klinedinst DB, Yilgor E, Yilgor I, Beyer FL, Sheth JP, Wilkes GL. Rubber Chemistry and Technology 2005;78:737–53.
[17] Sheth JP, Klinedinst DB, Pechar TW, Wilkes GL, Yilgor E, Yilgor I. Macromolecules 2005;38:10074–9.
[18] Sheth JP, Klinedinst DB, Wilkes GL, Yilgor I, Yilgor E. Polymer 2005; 46:7317–22.
[19] Sheth JP, Wilkes GL, Fornof A, Long TE, Yilgor I. Macromolecules 2005;38:5681–5.
[20] Yilgor I, Yilgor E, Guclu G, Ward TC, Wilkes GL. Polymer 2006;47: 4105–14.
[21] Dreyfuss P, Dreyfuss M, Pruckmayr G. Encyclopedia of polymer science and engineering. New York, NY: Wiley Interscience Publication; 2000.
[22] Abouzahr S, Wilkes GL. Polymer Preprints 1980;21:193–4.
[23] Das S, Yilgor I, Yilgor E, Toki H, Hsiao B, Wilkes GL, in preparation.
[24] Pan N. Science and Engineering of Composite Materials 1996;5:63–72.
[25] Selbertinger E, Ziche W. EP 1,496,079 (Wacker Chemie AG); 2004.